# Interface roughness of InAs/AlSb superlattices investigated by x-ray scattering

B. Jenichen[a)]
*Paul-Drude-Institut für Festkörperelektronik, Hausvogteiplatz 5-7, Berlin D-10117, Germany*

S. A. Stepanov
*MPG AG "Röntgenbeugung," Hausvogteiplatz 5-7, Berlin D-10117, Germany*

B. Brar and H. Kroemer
*Department of Electrical and Computer Engineering, University of California, Santa Barbara, California 93106*

(Received 28 June 1995; accepted for publication 18 September 1995)

InAs/AlSb short period superlattices grown either with AlAs-like or with InSb-like interfaces are investigated by grazing incidence x-ray scattering and high resolution diffractometry. The superlattices are grown on a relaxed AlSb buffer layer. It is shown that the two possible stackings of layers in the superlattices resulting in a different degree of lattice relaxation lead also to a different height of interface roughness. The lateral and vertical correlation lengths of the roughness decrease with increasing relaxation of the superlattice. The vertical correlation length corresponds to an almost complete correlation of different interfaces in the case of the nearly perfect superlattice with InSb-like interfaces. © *1996 American Institute of Physics.* [S0021-8979(96)04201-0]

## I. INTRODUCTION

The combination of InAs and AlSb offers interesting physical properties as the large conduction band offset and the high electron mobility in InAs.[1] The possibility of large electron sheet concentrations[2] leads to high-speed-device applications. Interface (IF) properties are of great importance for the structural, optical, and electrical quality of heterojunctions. Two different types of IF can be grown by molecular beam epitaxy in the InAs/AlSb system.[1] Fig. 1 displays the different stackings for the so called InSb-like and the AlAs-like IFs. When the InAs layer is terminated by In atoms and the AlSb layer begins with Sb atoms, an InSb-like IF is formed. The AlAs-like IF is realized, when the InAs layer ends with As atoms and the AlSb layer begins with Al atoms. The structural properties of the superlattices (SLs) investigated by different methods strongly depend on the type of IF above the AlSb layer.[3,4] The reason for these differences lies in the different degree of lattice relaxation of the metastable SL. The higher degree of relaxation of the SLs with AlAs-like IF is mainly caused by diffusion of As into the AlSb layers[5] during the process of formation of the IFs.

Recently, grazing incidence x-ray methods became a valuable tool to investigate roughness of surfaces and IFs in multilayers.[6–19] In the present work the interface roughness of partly relaxed short period superlattices (SL) is investigated by grazing incidence x-ray scattering. The influence of a different degree of relaxation of the SLs and the impact of the buffer layer on the interface roughness as well as on the lateral and vertical correlation lengths of the IF roughness are investigated. The limits of the present scattering theories for rough IFs are demonstrated.

[a)]Electronic mail: jen@pdi.wias-berlin.de

## II. EXPERIMENT

Samples consisting of a SL with 138 periods of 6 monolayers (ML) InAs and 6 ML AlSb on top of a 1 $\mu$m thick AlSb buffer layer were grown by molecular beam epitaxy (MBE) on a semi-insulating (001) GaAs substrate. The growth temperatures for the buffer layer and the SL were 600°C and 430°C, respectively. The AlSb layers were grown at 1 $\mu$m/h, and the InAs layers at 0.25 $\mu$m/h. The group-V-III beam flux ratio in both types of layers was 5:1. To force an InSb-like or AlAs-like IF formation, we provide either excess of Sb or As at the IF during the so-called soak time $\tau_s$.[1] For the sample with AlAs-like IF $\tau_s$ was chosen to be 3 s, while for the sample with InSb-like IF the Sb soak time was 5 s.

The measurements of grazing incidence x-ray scattering were performed with a diffractometer in double and triple crystal configuration (BEDE D3). The monochromator was a single channel cut crystal in combination with 1 mm slits resulting in the separation of the CuK$\alpha_1$-line. The angular divergence behind the monochromator was 0.003° and the angular acceptance of the detector was below 0.1°. The analyzer crystal used in some of the measurements was a channel cut silicon (111) with an angular acceptance of 0.003°. x-ray CuK$\alpha_1$ radiation ($\lambda = 0.154$ nm) from a rotating anode source (operated at 9 kW) was used. Longitudinal scans with and without sample offsets were recorded to distinguish between the diffuse scattering and the reflected intensity. The transverse scans were performed through several Bragg peaks of the SL and compared to the computer simulations of the diffuse scattering in order to determine the lateral correlation length of interface roughness of the SLs. Finally, longitudinal scans with the analyzer crystal were performed near the first superlattice peak to detect the vertical roughness correlation in the SL stack. For all scans, the sample was completely exposed to the incident beam leading to symmetric profiles of the diffuse scattering in the transverse scans.

 0021-8979/96/79(1)/120/5/$6.00 

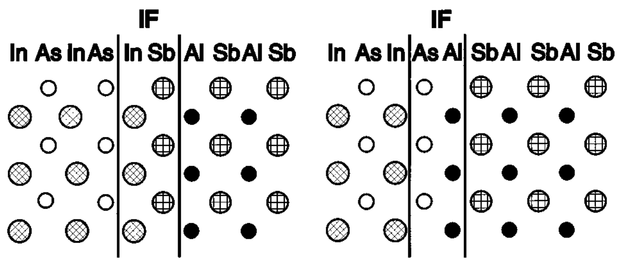


FIG. 1. Schematic view of the stacking near the InSb-like (left) and the AlAs-like (right) interfaces (IFs).

For the further characterization of the samples large angle, high resolution diffractometric measurements were performed[5] using the same diffractometer (BEDE D3) equipped with two asymmetrically cut grooved silicon crystals in (n,+n) setting[20,21] as a monochromator and with the analyzer described above. The diffraction curves were measured in the symmetric (004) and the asymmetric (115) reflections in order to measure the lattice parameter differences perpendicular and parallel to the layers. Triple crystal area scans were recorded near the AlSb buffer peak including the average lattice reflection of the SL (zero order satellite) in the (004) and (224) geometry.

## III. THEORY

Roughness of interfaces causes fluctuations $\delta\chi(\mathbf{r})$ of the polarizability in the scattering object and thereby gives rise to a non-specular diffuse scattering of x-rays at grazing incidence. The most recognized approach to calculate this effect in the lowest order over the perturbation $\delta\chi(\mathbf{r})$ is to apply the reciprocity theorem and the distorted wave Born approximation. This approach first used by Sinha *et al.*[6] for the scattering from a rough surface, has been extended for multilayers and superlattices.[10,12,14,15,19,22] The differential cross section of diffuse scattering per unit solid angle is:

$$\frac{d\sigma}{d\Omega}=\langle|f|^2\rangle, \tag{1}$$

where $\langle\ldots\rangle$ denotes averaging over the fluctuations and $f$ the amplitude of diffuse scattering calculated using the reciprocity theorem and distorted wave Born approximation

$$f=\frac{k^2}{4\pi}\int d^3\mathbf{r}\mathbf{E}^{\rm out}(\mathbf{r})\,\delta\chi(\mathbf{r})\mathbf{E}^{\rm in}(\mathbf{r}). \tag{2}$$

The parameter $k$ is the modulus of the wave vector $\mathbf{k}$ of x-rays in vacuum, and $\mathbf{E}^{\rm in}(\mathbf{r})$ and $\mathbf{E}^{\rm out}(\mathbf{r})$ are the wavefields inside the sample produced by the x-ray plane waves coming from the incidence direction and from the observation point, respectively. These wavefields can be determined considering the boundary conditions for x-rays at each interface. For multilayers, the well-known methods are the Parrat's recurrent formulae[23,24] and the Abeles matrix method.[25] Substituting the wavefields into the equations (1) and (2) one can find

$$\frac{d\sigma}{d\Omega}=\left(\frac{k^2}{4\pi}\right)^2\sum_{j,k=1}^{N}\sum_{l,m,p,q=1}^{2}\langle\delta\chi_j(\mathbf{Q}^j_{lm})\,\delta\chi^*_k(\mathbf{Q}^k_{pq})\rangle, \tag{3}$$

where $\mathbf{Q}^j_{lm}=\mathbf{K}^{j\ \rm out}_l+\mathbf{K}^{j\ \rm in}_m$ is the wave vector transfer, $\Sigma_{j,k}$ denotes the summation over the interfaces and $\Sigma_{l,m,p,q}$ the summation over the transmitted and reflected waves in multilayers. The quantities $\delta\chi_j(\mathbf{Q}_{lm})$ are the Fourier transforms of $\delta\chi(\mathbf{r})$. Rough interfaces are commonly treated as sharp boundaries with random displacements $u_j(\boldsymbol{\rho})$ from their mean position $z_j$ and step-wise changes in x-ray polarizabilities. With this approximation the average in equation (3) can be expressed[15,19] in terms of the root mean square (rms) displacement of interfaces, $\sigma_j^2=\langle u_j^2(\boldsymbol{\rho})\rangle$, and the displacement–displacement correlation functions $\mathcal{K}_{jk}(\boldsymbol{\rho})=\langle u_j(0)u_k(\boldsymbol{\rho})\rangle$

$$\frac{d\sigma}{d\Omega}=S\left(\frac{k^2}{4\pi}\right)^2\sum_{j,k=1}^{N}\sum_{l,m,p,q=1}^{2}\frac{\Delta\chi_j\Delta\chi_k}{Q^j_{lmz}Q^{k*}_{pqz}}\times e^{-i(Q^j_{lmz}z_j-Q^{k*}_{pqz}z_k)-(Q^{j2}_{lmz}\sigma_j^2+Q^{k*2}_{pqz}\sigma_k^2)/2}\times\int d^2\boldsymbol{\rho}\,e^{-i\mathbf{q}\boldsymbol{\rho}}\{e^{Q^j_{lmz}Q^{k*}_{pqz}\mathcal{K}_{jk}(\boldsymbol{\rho})}-1\}. \tag{4}$$

Here $S$ denotes the illuminated area of the sample and $\mathbf{q}$ is the lateral component of vectors $\mathbf{Q}_{lm}$. This component is the same for all $\mathbf{Q}_{lm}$ because the lateral component of wave vectors is not changed at specular reflection and refraction.

There is a variety of suggestions[6,10,15,17,19] on the form of the correlation function $\mathcal{K}_{jk}(\boldsymbol{\rho})$. Here, we used the function derived in Ref. 19 and corresponding to the model in Ref. 11 for the roughness transfer and accumulation during subsequent growth of multilayers

$$\mathcal{K}_{jk}(\boldsymbol{\rho})=\sum_{n=\max(j,k)}^{N}\sigma_n^2\frac{\xi_n^2}{\xi_n^2+p_n^2}\exp\left[-\frac{\boldsymbol{\rho}^2}{\xi_n^2+p_n^2}\right]. \tag{5}$$

$p_n^2=4\nu(2z_n-z_j-z_k)$ and $\nu$ is a diffusion-like relaxation parameter of roughness. The parameters $\sigma_n$ and $\xi_n$ are the rms height and the lateral correlation length, respectively, of roughness *acquired* during the formation of the $n$-th interface in addition to the roughness already transferred from deeper IFs. The rms of the transferred roughness decreases $\sigma_n'=\sigma_n/\sqrt{1+p_n^2/\xi_n^2}$ and the wavelength of transferred roughness increases with the spacing between the interfaces. In the limit $\nu\rightarrow\infty$, $\mathcal{K}_{j\neq k}(\boldsymbol{\rho})=0$, i.e., roughness transfer and correlations are absent. In the opposite limit $\nu\rightarrow 0$, the roughness is completely transferred and accumulated as in Ref. 15. For $\sigma_{n<N}=0$ and $\sigma_N\neq 0$ the roughness of the substrate is transferred to all interfaces. This is the complete correlation limit of the model in Ref. 10.

In addition we assume all $\xi_n$ to be equal and introduce the vertical correlation length of roughness $\xi_{\rm vert}=\xi^2/\nu$. Equation (4) was integrated over the component of vector $\mathbf{q}$ perpendicular to the plane of specular reflection because of the large height of receiving slit in the experiment. The specular x-ray reflectivity was simulated with the help of a computer program described elsewhere.[24]

## IV. RESULTS

Fig. 2 shows the longitudinal scans of the reflected intensity (squares) and the diffuse scattering (circles). The diffuse scattering is clearly observed in scans with an angular

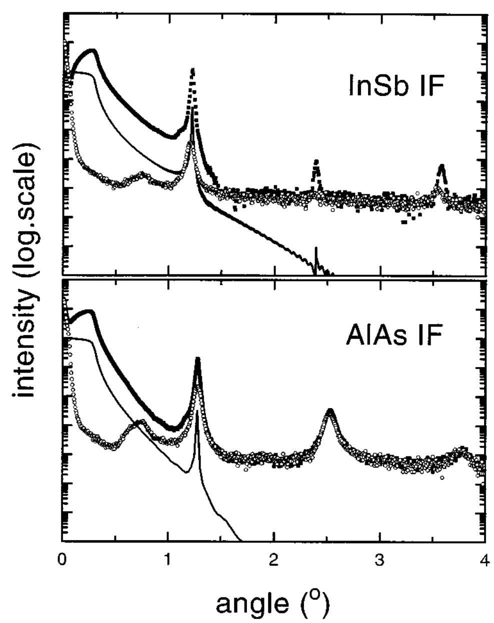


FIG. 2. Measured reflectivity (squares), calculated reflectivity (line), and diffuse scattering (points, measured with 0.5 degrees offset) of samples with InSb-like (top) and AlAs-like (bottom) interfaces (IFs). For the calculations the rms roughnesses of each IF were assumed to be 0.6 nm and 1.0 nm, respectively.

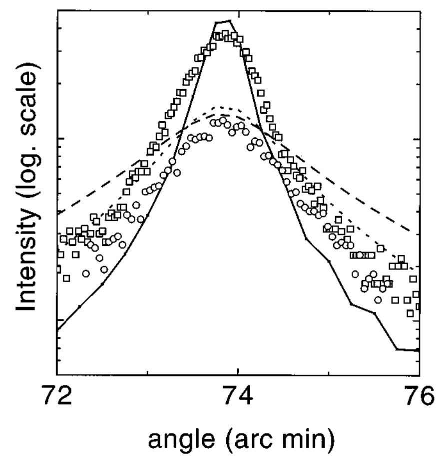


FIG. 3. Longitudinal $\theta/2\theta$ scans with sample offset 0.1° through the first superlattice maximum taken with the analyzer crystal for samples with InSb-like (squares) and AlAs-like (circles) interfaces. Theoretical calculations for complete vertical correlation (line) and a correlation length of 100 nm are given for comparison (dashed line for 0.6 nm rms roughness and dotted line for 1.0 nm rms roughness).

offset of the sample of 0.5°. The reflected beam and the diffuse scattering show pronounced Bragg peaks of the SL. These maxima in the diffuse scattering testify that the roughness of the IFs is correlated.[7–10,15–17,19]

From the comparison of the corrected x-ray reflectivity with the computer simulations (Fig. 2) the averaged rms roughness was obtained (Table I). The rms roughness is higher for the sample with AlAs-like IF than for the sample with InSb-like IF. In both cases, theory and experiment differ at the large-angle part of the curves. This discrepancy is due to the large rms roughness which for large angles is beyond the limits of the algorithm.[24] The applicability of this algorithm as well as of the diffuse scattering model described in the previous section requires $\sigma Q \ll 2\pi$, or $\alpha_i \ll \lambda/2\sigma$, where $\alpha_i$ is the incidence angle and $\lambda$ is the x-ray wavelength.

We should note that the effect of roughness on the specular reflectivity is basically not distinguishable[6,26] from that of the transition layers with a thickness of $t_{tr}=2\sigma$. The presence of transition layers in InAs/AlSb superlattices caused by interdiffusion has been proven in Ref. 4. However, the transition layers do not result in non-specular diffuse scattering.

TABLE I. Results obtained from the comparison of longitudinal and transverse scans to the corresponding calculations in the distorted wave Born approximation. The average relaxation of the superlattices was obtained from high resolution diffractometry.[a]

| IF | InSb-like | AlAs-like |
|---|---|---|
| rms-roughness [nm] | 0.6 | 1.0 |
| Lateral correlation length [nm] | 140 | 100 |
| Vertical correlation length [nm] | 400-500 | 100-400 |
| Relaxation of SL on AlSb [%] | 30 | 91 |

[a]See Ref. 5.

Figs. 3 and 4 display the longitudinal and transverse scans through the first SL maxima. These scans record the nonspecular x-ray scattering and contain information about the vertical and lateral correlation lengths of the interface roughness. These correlation lengths have been obtained by comparing the numerical calculations with the experimental data (Table I).

First, the analysis of the longitudinal scans taken with an analyzer crystal proves that the vertical correlation length of roughness in both cases is of the order of the total thickness of the SL, $\xi_{vert} \simeq 500$ nm. The dotted and the dashed lines in Fig. 3 show the theoretical curves for $\xi_{vert} \simeq 100$ nm and the rms roughnesses of 0.6 nm and 1.0 nm, respectively, which are considerably wider than the corresponding experimental curves. Obviously the vertical correlation length of the sample with InSb-like IFs is larger than that of the sample with AlAs-like IFs. For the simulation of the transverse scans, the averaging over the exit angles due to the low resolution of the receiving slit of the detector was taken into account. The large width of the curve in the transverse scan for the sample with AlAs-like interfaces points to the small lateral correlation length (to the short lateral "wavelength") of roughness in this case.

A discrepancy between the distorted wave Born approximation and the experiment arises for the higher order SL maxima. Therefore only the experimental results for the higher order satellites are presented. An adequate theoretical description is still missing (see section III). The average relaxation of the SL with respect to the AlSb buffer layer is also given in Table I for comparison. The average SL relaxation was obtained from high resolution diffractometry comparing the symmetric (004) and asymmetric (115) and (224) reflections.[5]

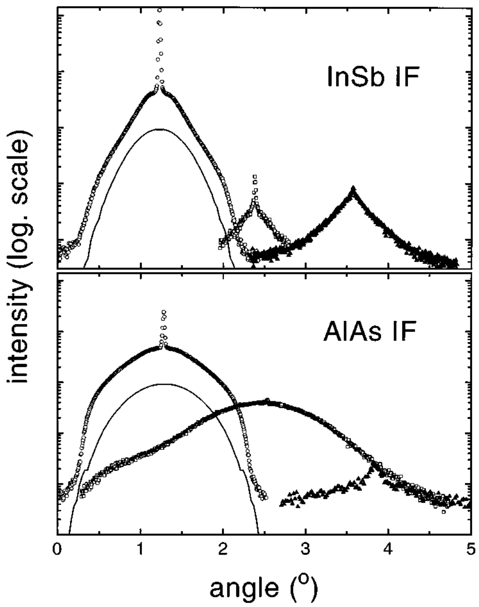


FIG. 4. Transversal scans through the first three Bragg peaks of the superlattice (first: points, second: squares, third: triangles) of samples with InSb-like (top) and AlAs-like (bottom) interfaces (IFs). Calculations are shown (with vertical offset) for the first maximum and lateral correlation lengths of 140 nm and 100 nm, respectively.

## V. DISCUSSION

The AlSb buffer layer is almost totally relaxed,[4,5] i.e., the misfit dislocation density near the interface to the substrate is higher than $10^6 cm^{-1}$ (see Ref. 27). This high dislocation density is inhomogenously distributed, leading to a certain surface roughness due to steps connected with the dislocation gliding[28] and to inhomogenous strains in the layer.

The relaxation of the SL with InSb-like IFs is relatively low, and only a few additional defects are introduced by the SL itself. Therefore the vertical correlation length of the IF roughness amounts to about 500 nm, which is in fact the whole thickness of the SL. Triple crystal scans also yield coherently scattering domains, with sizes of the order of the SL thickness.

The relaxation of the SL with AlAs-like IF is strong and inhomogenous with depth.[5] The amount of crystal defects introduced by the SL is large[4] leading to a higher value of the rms roughness and to a reduction of the lateral and vertical correlation lengths of the IF roughness.

The theoretical model applied to the simulations of diffuse scattering contains some assumptions which are not completely adequate for samples with thin layers and large rms roughness especially in the range of large angles. Firstly, it is assumed that the layers have constant composition and density within their thickness and sharp interfaces randomly shifted up and down along the lateral coordinates. This is not strictly correct for SLs where the transition domains are comparable with the thickness of the layers. Secondly, it is assumed that the x-ray wavefields are not considerably changed within the rms roughness. This condition is not fulfilled when the rms roughness is of the same order as the thickness of the layers. Thus, the numerical results given in Table I must be treated with some care and a further development of the theory of diffuse scattering is needed.

## VI. CONCLUSIONS

The roughness of short period SLs exhibiting a different degree of relaxation has been investigated in detail. Due to surface steps introduced by the glide of misfit dislocations and inhomogenous strains connected with the inhomogenous distribution of misfit dislocations the surface of the buffer layer introduces roughness of the interfaces of the growing SL. This roughness is highly correlated vertically, when the SL grows, without introducing additional crystal defects. The SL with InSb-like IFs is a good example for such a case. However, in the SL with AlAs-like IFs both the vertical and the lateral correlation lengths are reduced and the rms roughness is increased by introducing a relatively high density of additional crystal defects such as misfit dislocations and stacking faults.

## ACKNOWLEDGMENTS

The authors thank H. Grahn and G. Jungk for helpful discussions.

[1] G. Tuttle, H. Kroemer, and J. H. English, Appl. Phys. Lett. **67**, 3032 (1990).
[2] C. Nguyen, B. Brar, H. Kroemer, and J. H. English, J. Appl. Phys. **73**, 8313 (1993).
[3] B. Brar, J. Ibbetson, H. Kroemer, and J. H. English, Appl. Phys. Lett. **64**, 3392 (1994).
[4] J. Spitzer, A. Höpner, M. Kuball, M. Cardona, B. Jenichen, H. Neuroth, B. Brar, and H. Kroemer, J. Appl. Phys. **77**, 811 (1995).
[5] B. Jenichen, H. Neuroth, B. Brar, and H. Kroemer, in *Strained Layer Epitaxy – Materials, Processing, and Device Applications*, Mater. Res. Soc. Proc., edited by J. Bean, E. Fitzgerald, J. Hoyt, and K. Y. Cheng (MRS, Pittsburgh, PA, 1995), to be published.
[6] S. K. Sinha, E. B. Sirota, S. Garoff, and H. B. Stanley, Phys. Rev. B **38**, 2297 (1988).
[7] D. E. Savage, J. Kleiner, N. Schimke, Y.-H. Phang, T. Jankowski, J. Jacobs, R. Kariotis, and M. G. Lagally, J. Appl. Phys. **69**, 1411 (1991).
[8] Y. H. Phang, D. E. Savage, T. F. Kuech, M. G. Lagally, J. S. Park, and K. S. Wang, Appl. Phys. Lett. **60**, 2986 (1992).
[9] Y. H. Phang, D. E. Savage, R. Kariotis, and M. G. Lagally, J. Appl. Phys. **74**, 3181 (1993).
[10] Z. H. Ming, A. Krol, Y. L. Soo, Y. H. Kao, J. S. Park, and K. L. Wang, Phys. Rev. B **47**, 16373 (1993).
[11] E. Spiller, D. Stearns, and M. Krumrey, J. Appl. Phys. **74**, 107 (1993).
[12] V. Holý, J. Kuběna, I. Ohlídal, K. Lischka, and W. Plotz, Phys. Rev. B **47**, 15896 (1993).
[13] D. Bahr, W. Press, R. Jebasinski, and S. Mantl, Phys. Rev. B **47**, 4385 (1993).
[14] S. K. Sinha, J. Phys. III France **4**, 1543 (1994).
[15] V. Holý and T. Baumbach, Phys. Rev. B **49**, 10669 (1994).
[16] T. Salditt, T. H. Metzger, and J. Peisl, Phys. Rev. Lett. **73**, 2228 (1994).
[17] J.-P. Schlomka, M. Tolan, L. Schwalowsky, O. H. Seeck, J. Stettner, and W. Press, Phys. Rev. B **51**, 2311 (1995).
[18] D. K. G. de Boer, Phys. Rev. B **51**, 5297 (1995).
[19] V. M. Kaganer, S. A. Stepanov, and R. Köhler, Phys. Rev. B (1995), to be published.
[20] W. Du Mond, Phys. Rev. **52**, 872 (1937).
[21] W. J. Bartels, J. Vac. Sci. Technol. **1**, 338 (1983).
[22] A. V. Andreev, A. G. Michette, and A. Renwick, J. Modern Optics **35**, 1667 (1988).

[23] L. G. Parratt, Phys. Rev. **95**, 359 (1954).
[24] M. Wormington, D. K. Bowen, and B. K. Tanner, in *Structure and Properties of Interfaces in Materials*, No. 238, in Mat. Res. Soc. Proc., edited by W. A. T. Clark, U. Dahmen, and C. L. Briant (MRS, Pittsburgh, PA, 1992), pp. 119–124.
[25] F. Abeles, Ann. Phys. (Paris) **3**, 504 (1948); **5**, 596 (1950).
[26] S. A. Stepanov and R. Köhler, J. Appl. Phys. **76**, 7809 (1994).
[27] S. N. G. Chu, A. T. Macrander, K. E. Strege, and D. W. Johnston, J. Appl. Phys. **57**, 249 (1985).
[28] N. Frank, G. Springholz, and G. Bauer, Phys. Rev. Lett. **73**, 2236 (1994).